Numerical Study of Effects of injection pressure and location of secondary injection inside low-thrust satellite nozzle

Ajmal Baig, Ali Ahmed, S. Zahir

National Engineering and Scientific Commission, Islamabad, Pakistan

Abstracts

Convergent-Divergent Nozzle is normally used for thrust generation. A useable control force can be generated at the expanse of some thrust loss as soon as the secondary jet interacts with the flow through the nozzle. Secondary injection in the divergent section of the nozzle diverts the mainstream flow and causes a static pressure change on the nozzle wall. This jet interaction produces an asymmetric static pressure distribution on the opposite walls of the nozzle with respect to the centre line of the nozzle. The pressure distribution depends upon the location of injection and injection pressure. Computational results are obtained as non-dimensional static pressure on the divergent section of the nozzle and depth of jet penetration (Y/D) for variation in secondary injection pressure (P_{inj}/P_i) and injection location (X/L). These computations are done using the Navier-Stokes Equations and control volume techniques.

Nomenclature

A_e = nozzle exit area
A_i = nozzle inlet area
A_T = nozzle throat area
D_{jet} = injection orifice diameter
D_T = nozzle throat diameter
D = nozzle exit diameter
L = axial length from throat to exit of nozzle
P_b = design back pressure
P_i = nozzle inlet pressure
P_{inj} = secondary injection pressure
P_d = static pressure integrated on divergent section of nozzle wall
X = distance from throat along nozzle wall
Y = gross jet penetration

Introduction

Secondary fluid injection inside the nozzle is one method used for producing control force for space vehicles. This technique uses asymmetric wall forces caused by lateral injection of a fluid (gas or liquid) into the divergent portion of the supersonic exhaust nozzle. In addition to the usual jet reaction, local high pressures associated with an induced shock wave "amplify" the jet reaction. Experiments on secondary injection had been reported by Hausmann et al [1] and they demonstrated that the shock-induced reaction associated with an air jet directed into supersonic air (both gases at ambient temperature) could be as large as the jet reaction. The nature of this shock-induced reaction and the way in which it depends upon the mainstream and injectant properties have since been the subject of considerable study, mostly experimental. Several experiments have been reported for jet-interference phenomena on simple aerodynamic surfaces [2-6]. The initial studies of secondary injection [7-9] used gases as the injected fluids.

A preliminary work was done to study the secondary injection as an air into the main stream of fluid passing through the throat to the divergent section of the nozzle. Initially the study is focused to understand the phenomenon of secondary injection in the divergent section and flow behavior before and aft the injection location. In the present CFD study, a shock wave is produced in cases of supersonic jet injections with flow separation. In these cases there is circulation of flow downstream of the point of injection causing redeflection of mainstream flow as well. Mach distributions along the plane of injection show that the major affect of injection is down stream of flow and a very little effect is on the upstream. This change in flow velocity downstream of the injection creates an asymmetric pressure distribution on the wall of the nozzle.

Geometry of Nozzle and Injector

A convergent-divergent nozzle of expansion ratio A_e/A_T = 9.0 with a conical divergent section was used. The mainstream nozzle flow as well as the injection jet flow had same fluid properties of ideal gas at γ = 1.4. The injector is of circular shape with diameter ratio given as D_{jet}/D_{throat} = 0.02. The injector was located at 5 coplanar locations, axially along the nozzle divergent wall at X/L = 0.1, 0.3, 0.5, 0.7 and 0.9.

Grid Generation

A 3D-structured grid was used consisting of 2 blocks; one comprising of the main nozzle and the other was that of a tube inserted to accommodate injection orifice into the main nozzle grid. The study is done in a series of CFD simulations for various cases of the same nozzle by varying, two parameters: 1) the position of injection orifice, from the throat and 2) the injection jet pressure, P_{inj} .The grid varying parameter was the location of injector, along the length of the nozzle wall. Injection tube was placed at 5 coplanar locations axially along the nozzle wall. Fig.1 shows the side view of the nozzle grid with injection point at X/L = 0.5. Clustering is done at injection location. Fig.2 shows the isometric view of full-section nozzle grid, inside is the close-up showing the injection tube block.

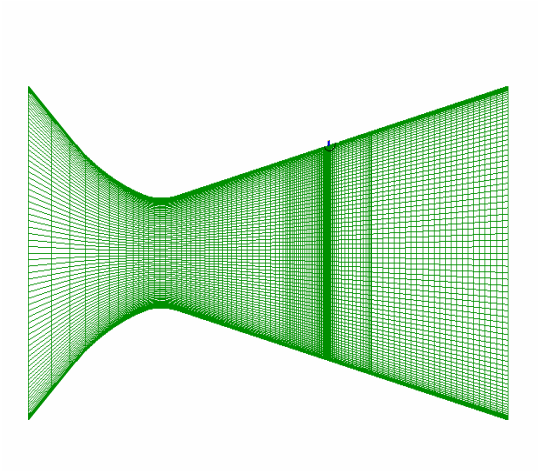

Figure 1: Side view of Nozzle Grid at X/L=0.5

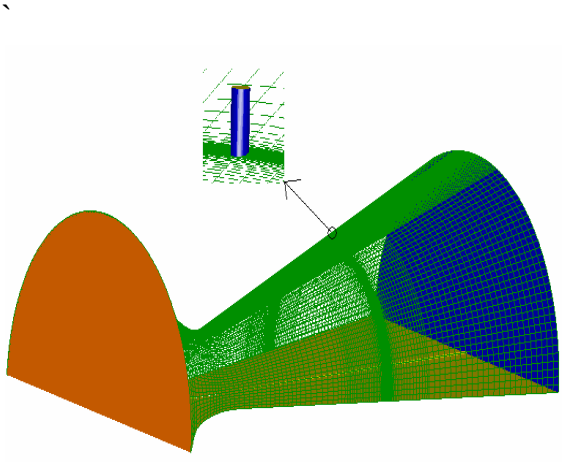

Figure 2: Grid of full-section of nozzle and Close-up of Injection tube at X/L=0.5

Grid Independence

In order to optimize the results, grid adaption in the solver was done for regions with high flow gradients and around injector location. The flow gradients of focus were that of mach no. at and above sonic value. This was done to capture the shock that was anticipated for sonic jet injections and separation region upstream and downstream

of the. Grid adaption is a add-on feature in the solver used and this adaption strategy has allowed for the study to be grid independent.

Governing Equations

A 3D coupled explicit model was used. The system of governing equations for a single-component fluid, written to describe the mean flow properties, is cast in integral Cartesian form for an arbitrary control volume V with differential surface area dA as follows:

$$\frac{\partial}{\partial t}\int_v W.dV + \oint [F - G]dA = \int_V H.dV$$

Where the vectors W , F , and G are defined as :

$$W = \begin{Bmatrix} \rho \\ \rho u \\ \rho v \\ \rho w \\ \rho E \end{Bmatrix}, \qquad F = \begin{Bmatrix} \rho v \\ \rho vu + p\hat{i} \\ \rho v + p\hat{j} \\ \rho vw + p\hat{k} \\ \rho vE + pv \end{Bmatrix},$$

$$G = \begin{Bmatrix} 0 \\ \tau_{xi} \\ \tau_{yi} \\ \tau_{zi} \\ \tau_{ij}v_j + q \end{Bmatrix}$$

The vector H contains source terms such as body forces and energy sources. Here ρ, v, E, and **p** are the density, velocity, total energy per unit mass, and pressure of the fluid, respectively. τ is the viscous stress tensor, and **q** is the heat flux.

Total energy E is related to the total enthalpy H by

$$E = H - p/\rho$$ Where

$$H = h + |v|^2/2$$

Turbulent Model

A single equation turbulent Spalart-Almaras was used. The transported variable in the Spalart-Almaras model, $\tilde{\nu}$, is identical to the turbulent kinematic viscosity except in the near-wall (viscous- affected) region. The transport equation for $\tilde{\nu}$ is

$$\frac{\partial}{\partial t}(\rho\tilde{\nu}) + \frac{\partial}{\partial x_i}(\rho\tilde{\nu}u_i) = G_\nu + \frac{1}{\sigma_{\tilde{\nu}}}\left[\frac{\partial}{\partial x_j}\left\{(\mu + \rho\tilde{\nu})\frac{\partial\tilde{\nu}}{\partial x_j}\right\} + C_{b2}\rho\left(\frac{\partial\tilde{\nu}}{\partial x_j}\right)^2\right] - Y_\nu + S_{\tilde{\nu}}$$

where **Gν** is the production of turbulent viscosity and Y_ν is the destruction of turbulent viscosity that occurs in the near-wall region due to wall blocking and viscous damping. σ_y and C_{b2} are constants and ν is the molecular kinematic viscosity. S_ν is a user-defined source term.

Solver Controls

The discritization for both flow and turbulent model was set at second degree with an initial CFL number of 0.1, which was gradually increased to 2.5 till convergence was achieved.

Results and Discussion

Penetration depth of Injection jet

In the previous study [10] it was observed that the penetration depth increases with the increase in the injection pressures for the given locations for the pressure ratio (P_{inj}/P_i) from 0.32 to 0.44. In the present study, the pressure ratio (P_{inj}/P_i) has been increased to 0.48 for all the given injection locations.Fig.3 shows the penetration depth (Y/D) variation with injection pressure (P_{inj}/P_i). Consider the graph in Fig.3 for penetration at X/L = 0.5, whereas the injection pressure (P_{inj}/P_i) was increased from 0.32 to

0.48 and it was seen that there was a nominal increase in the penetration depth of the jet from Y/D = 0.005 to 0.023 respectively. This increase in jet penetration is simply due to the increase in injection pressure and similar trend can be seen for the jet location (X/L) of 0.3. However as the jet location is moved at X/L = 0.7, a change in trend can be seen for injection pressures equal and greater than 0.4. Consider the depth variation curve for location X/L = 0.7 which shows that the trend is similar to X/L =0.5 till P_{inj}/P_i = 0.4 after which the penetration depth increases dramatically. The reason is the formation of induced shock wave due to the interaction of supersonic jet injection and the mainstream supersonic flow as shown in Fig.9. The sonic jet is formed when the local static pressure of the mainstream flow has decreased considerably due to expansion in nozzle divergent section. The expansion increases the difference between injection pressure and mainstream pressure. It is noticed that for the injection pressure (P_{inj}/P_i) 0.44 the jet Mach no. is subsonic at X/L = 0.3 and 0.5 and becomes supersonic at X/L = 0.58 as shown in Fig.4. For the injection pressure (P_{inj}/P_i) of 0.48, the jet mach becomes supersonic at X/L = 0.48 as shown in Fig.4. It should be further noted that the depth of penetration at X/L = 0.9 is more than at 0.7 due to the early formation of shock wave at P_{inj}/P_i = 0.36 and also due to an increase in the strength of shock. This increase in shock strength is explained by the Rankine-Hugonoit curve [11], which shows that stronger shocks are formed as the mainstream mach no is increased. The shock also creates separation of flow downstream of the mainstream flow. The penetration of the injected jet inside the main supersonic stream of fluid is shown in Figs.6-9 .the penetration of the secondary jet increases with the increase of injection pressure.

Pressure distribution on nozzle wall surface

The effect of the non-dimensional static pressure is also studied on the divergent section of the nozzle. The static pressure value depends upon the location of secondary injection for a particular value of injection pressure. The static pressure increases on the wall linearly with the increase of injection pressure for the location (X/L) of 0.3 as shown in Fig.5. This trend becomes nonlinear for the injection pressure (P_{inj}/P_i) greater than 0.44 for location (X/L) of 0.3. The effect of injection pressure is linear upto P_{inj}/P_i = 0.4 as the location of injection is changed from 0.3 to 0.5. At the jet locations downstream of the throat, the effective injection pressure value decreases and consequently the static pressure value also decreases .as a result effective control force on the body also decreases. For the location (X/L) of 0.9, the effective injection pressure is about 0.35.

The reason of this change of linearity to non-linearity is due to the circulation of flow downstream of the injection location. Note that the circulation in the separated flow is in the anti-clockwise direction as shown in Fig. 10 and Fig. 11 and it compels the mainstream flow to redeflect towards the nozzle wall due to which the mainstream flow regains its velocity and direction. Since the static pressure is inversely related to the velocity of the flow therefore the redirection of flow towards the wall surface reduces the affect of the strong penetration of the injection jets.

Conclusions

1. Since the mainstream mach no. increases downstream the divergent section of nozzle therefore the strength of the induced shock is greater as the injection location (X/L) is nearer to the exit. Hence the penetration depth also increases.
2. Static pressure distribution depends upon the injection pressure and the jet location (X/L).
3. Induced shocks give better penetration but the circulation aft the jet in the separated flow reduces the effect on the pressure distribution.

References

1. Hausmann, G. F. Thrust axis control of supersonic nozzles by air jet shock interference, *United Aircraft Corp*. Rept. R-63143-24 (May 2, 1952).
2. Amick, J. L. and Hayes, P. B. Interaction effects of side jets issuing from flat plates and cylinders alined with a supersonic stream, *Wright Air Dev. Div*. TR 60-329 (May 1960).
3. Liepman, H. P. On the use of side-jets as control devices, *ARS J*. 29,453-454 (1959).
4. Janos. J. J. Loads induced on a flat-plate wing by an air jet exhausting perpendicularly through the wing and normal to a free-stream flow of Mach number 2.0, *NASA* TN D-649 (March 1961).
5. Cubbison, R. W., Anderson, B. H., and Ward, J. J. Surface pressure distributions with a sonic jet normal to adjacent flat surfaces a t Mach 2.92 to 6.4, *NASA* TN D-580 (February 1961).
6. Romeo, D. J. and Sterrett, J. R. Aerodynamic interaction effects ahead of a sonic jet exhausting perpendicularly from a flat plate into a Mach number 6 free stream, *NASA* TN D-743 (April 1961).
7. Schweiger, M. K. Jet induced thrust vector control applied t o nozzles having large expansion ratios, *United Aircraft Corp., Hartford, Conn., Research Dept*. Rept. R-0937-33(March 1, 1957); confidential.
8. Bankston, L. T. and Larsen, H. M. Thrust vectoring bysecondary injection in the nozzle exhaust cone, *Bull. 15th Meeting, JANAF, Solid Propellant Group, Silver Spring*, Md.,SPIA 7,151-169 (June 1959).
9. Bankston, L. T. and Larsen, H. M. Thrust vectoring experiments: gas injection, *U. S. Naval Ordnance Test Station,China Lake, Calif., NAVORD* 6548, NOTS 2247 (May 28,1959).
10. Ali Ahmed, Ajmal Baig, S. Bilal, S. Zahir & M. A. Khan. Study of the effect of pressure and location of secondary injection inside supersonic nozzle, *4th IBCAST, Isamabad, Pakistan*, June, 2005.

M.Haluk Aksel and O. Cahit Eralp, *Gas Dynamics*, ed. 1992.

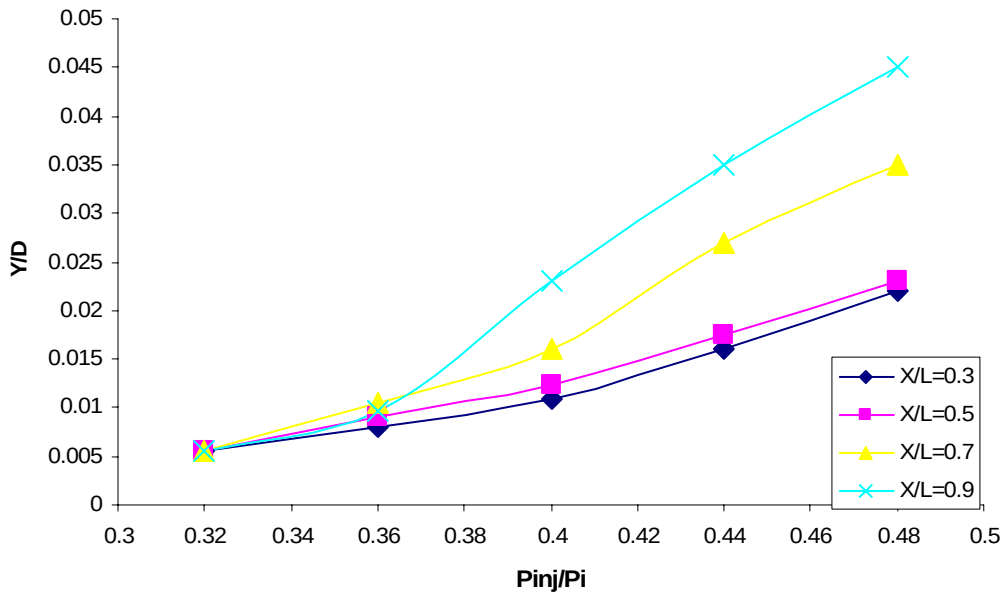

Figure 3: Penetration Depth vs Injection Pressure.

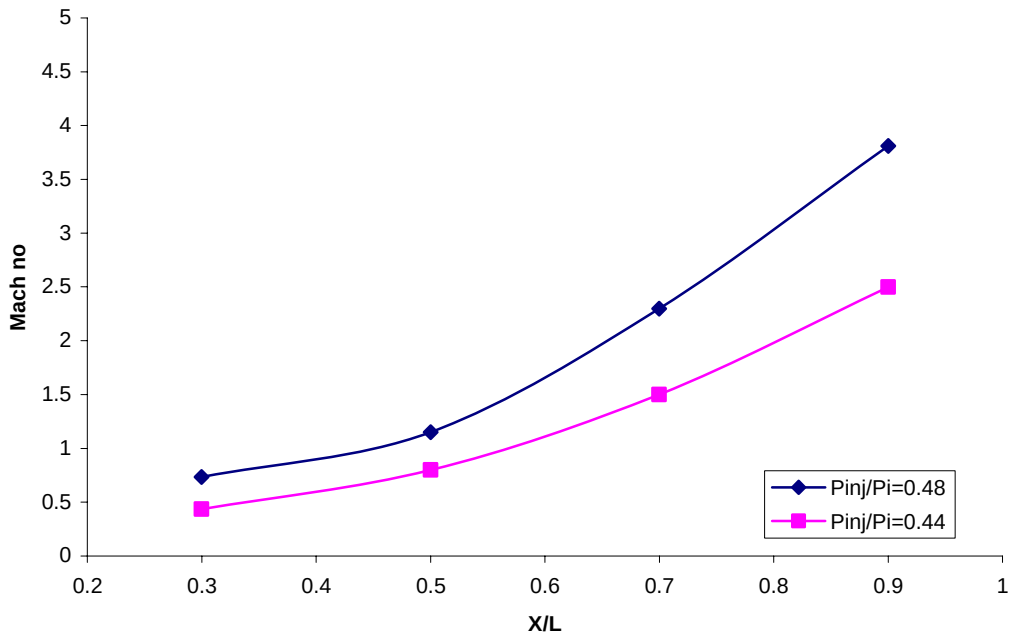

Figure 4: Mach no. vs injector locations (X/L) at P_{inj}/P_i = 0.44 and 0.48.

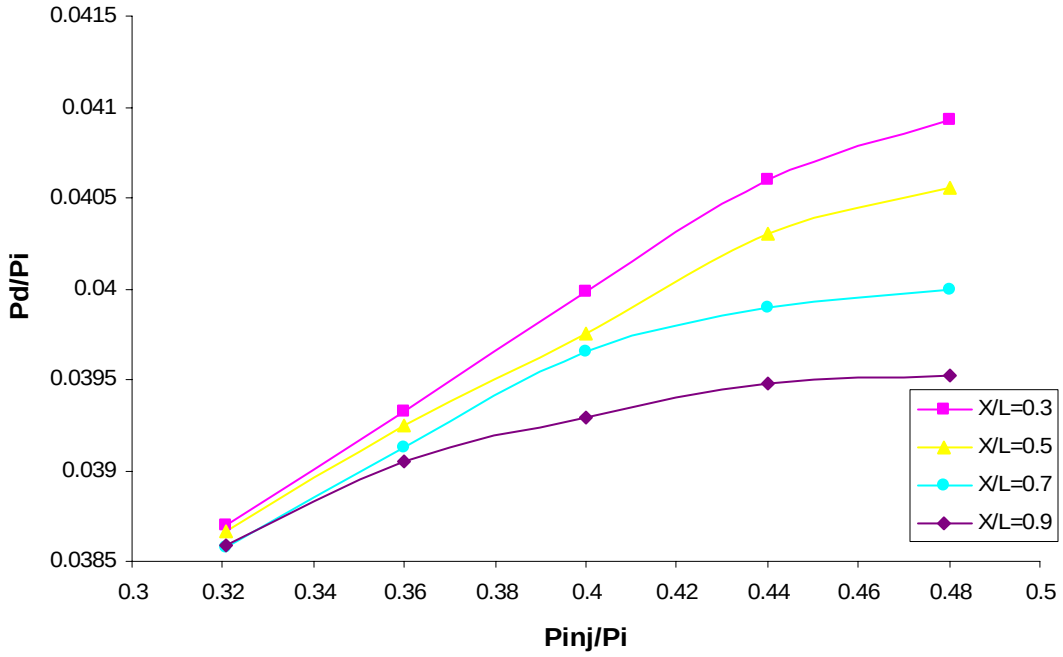

Figure 5: Static Pressure on Divergent wall section vs Injection Pressure.

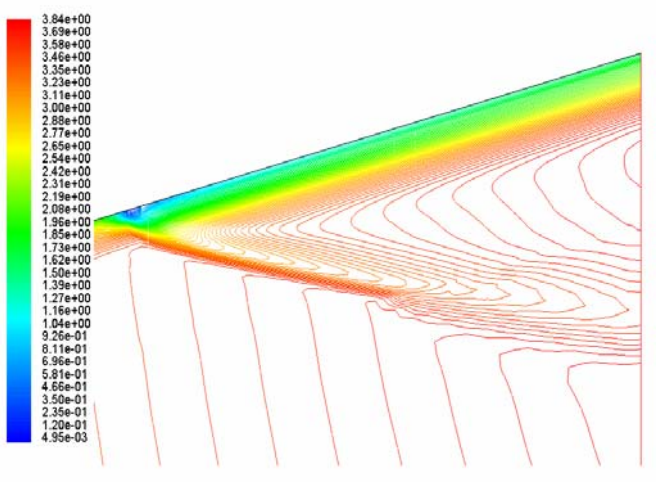

Figure 6: Mach contours - P_{inj}/P_i = 0.32 at X/L =0.7

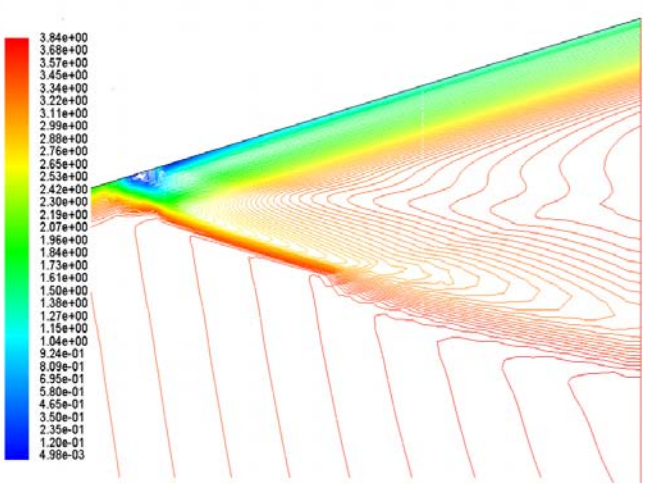

Figure 7: Mach contours - P_{inj}/P_i= 0.36 at X/L =0.7

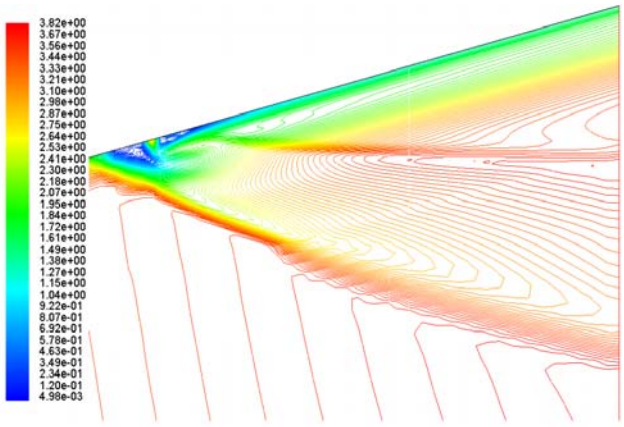

Figure 8: Mach contours - P_{inj}/P_i = 0.4 at X/L =0.7

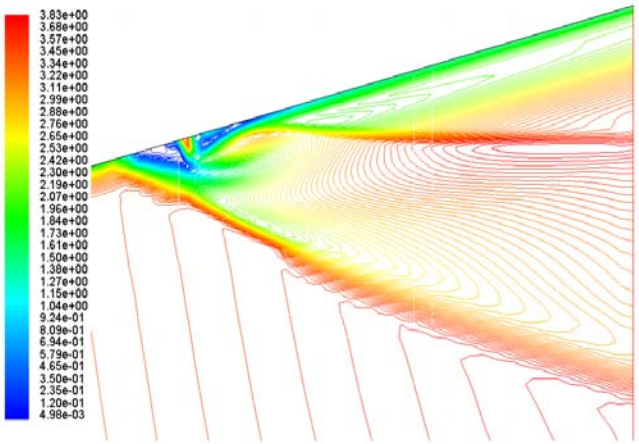

Figure 9: Mach contours - P_{inj}/P_i= 0.44 at X/L =0.7

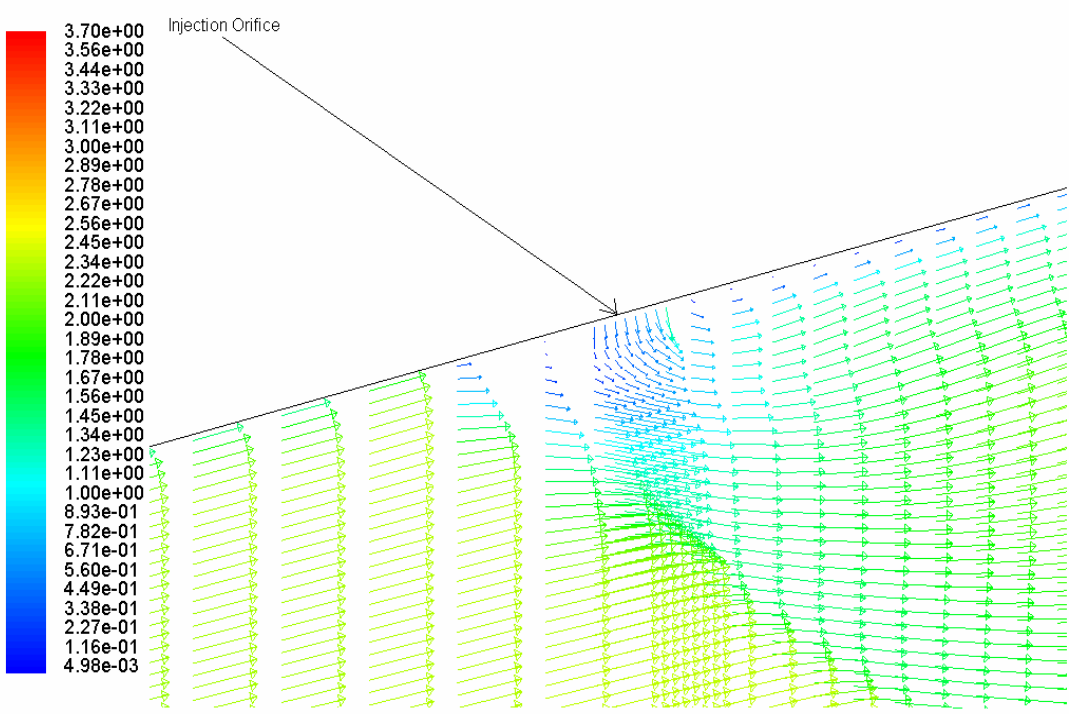

Figure 10: Mach distribution- Injection at X/L=0.3 and P_{inj}/P_i = 0.48

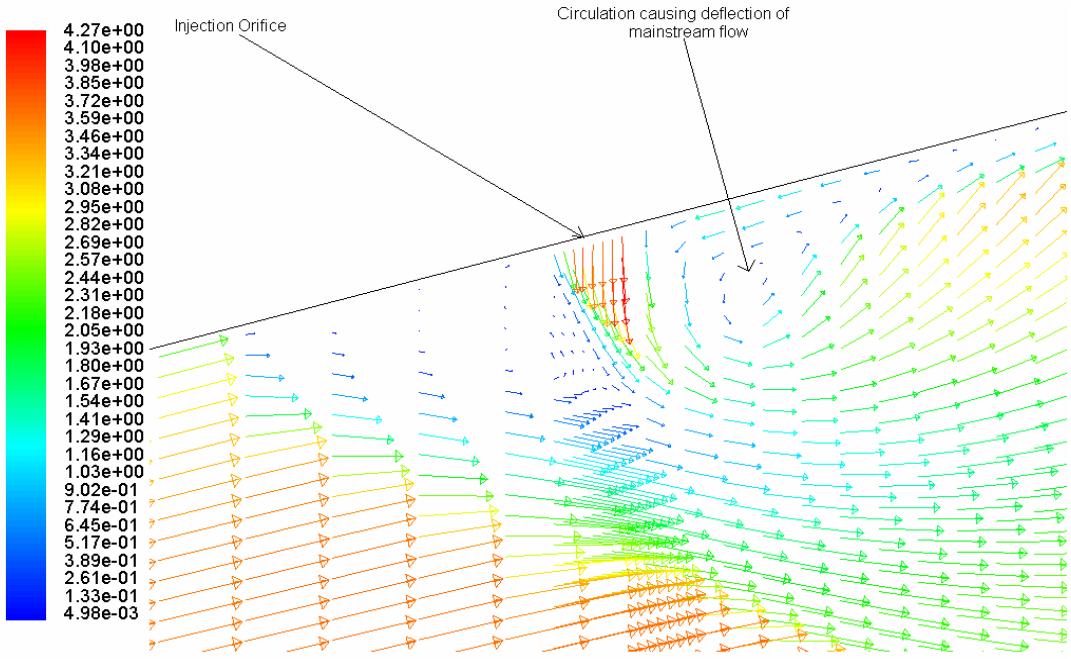

Figure 11: Mach distribution- Injection at X/L=0.9 and P_{inj}/P_i = 0.48